J. Min. Metall. Sect. B-Metall. 57 (2) (2021) 261 - 270

Journal of Mining and Metallurgy, Section B: Metallurgy

HARDNESS CHARACTERISTICS OF AS-CAST Ni-Ru-Zr ALLOYS

L. Chipise [a-d,*], N.R. Batane [b,d], P.K. Jain [b,e], S.H. Coetzee [b,f], B.O. Odera[b,g], W. Goosen[h], L.A. Cornish [a,b]

[a] University of the Witwatersrand, School of Chemical and Metallurgical Engineering and the DST-NRF Centre of Excellence in Strong Materials, Johannesburg, South Africa
[b] African Materials Science and Engineering Network (AMSEN: A Carnegie–IAS RISE Network)
[c] Manicaland State University of Applied Sciences, Mutare, Zimbabwe
[d] University of Botswana, Mechanical Engineering Department, Gaborone, Botswana
[e] University of Botswana, Physics Department, Gaborone, Botswana
[f] The Botswana Institute for Technology Research and Innovation, Gaborone, Botswana
[g] Technical University of Kenya, School of Mechanical and Process Engineering, Nairobi, Kenya
[h] Nelson Mandela University, Centre for High Resolution Transmission Electron Microscopy, Port Elizabeth, South Africa

(Received 07 March 2020; accepted 25 February 2021)

Abstract

The Vickers hardness of 21 as-cast Ni-Ru-Zr alloys of different compositions were studied, and nanohardness indentations were done on the individual phases. The results were used to explain the brittleness by assessing the proportions of the phases, and their morphologies. The compound hardness varied between 704 - 1289 HV, with ~$ZrRu_2$ being the hardest phase, and ~Zr_2Ni_7 being the least hard phase. The sample hardness was 300 - 1015 HV. Most of the samples were brittle, although there were regions of toughness around Ni_{36}:Ru_{13}:Zr_{51} and Ni_{20}:Ru_5:Zr_{75} (at.%). No alloy was identified to have potential good mechanical properties.

Keywords: *Hardness; Ni-Ru-Zr; Alloys; Ternary; As-cast*

1. Introduction

The Ni-Ru-Zr system is of interest because Ru and Zr can enhance properties of certain alloys. Ruthenium restrains the coarsening of γ' in the U720LI Ni-based superalloy [1], gives solid solution strengthening to Pt-based alloys [2], and improves the corrosion resistance of Ti alloys [3, 4]. Zirconium additions increase the creep resistance of Ni alloys [5]. Since solid solution strengthening is limited by the extent of the solid solutions, much interest has been shown in intermetallic compounds, either by themselves (e.g. Fleischer's work on intermetallic compounds [6,7]), or as components in alloys (e.g. the strengthening ~Ni_3Al precipitates in nickel-based superalloys [8], which is aided by the sloping (Ni) (where the brackets denote a solid solution) solvus that allows high proportions of ~Ni_3Al (where ~ denotes a phase based on that composition)). The Ni-Zr binary is a complex [9] with eight intermetallic compounds, while Ru-Zr has only two intermetallic compounds [10], and Ni-Ru none [11].

The Ni-Ru-Zr system had been studied with 21 different as-cast samples using SEM-EDX and identified with XRD, and the as-cast solid ranges and liquidus surface projections were drawn [12]. The samples were made by arc-melting [12], and their compositions were chosen to derive the phases within the ternary. As well as the extensions of the nine binary phases found, three ternary phases were identified: τ_1 $Zr_{24}Ru_{22}Ni_{44}$ (at.%), τ_2 $Zr_{74}Ru_4Ni_{22}$ (at.%), and τ_3 $Zr_{35}Ru_3Ni_{62}$ (at.%). Not all the binary phases were found, because some formed at lower temperatures. Table 1 lists the phases found (using the Pettifor order [13]).

The prior investigation on the phase diagram of Ni-Ru-Zr [12] gave an opportunity to study these phases, and measure their hardness and phase proportions in 21 samples to help explain the hardness variation of the different alloys, as was done by Hill et al. [14], and identify any potential alloys with good mechanical properties. Since there were several phases with different compositions and structures in the Ni-Ru-Zr system, (Table 1) [12], this gave an

Corresponding author: chipisel@gmail.com *

https://doi.org/10.2298/JMMB200307022C

Table 1. *Solid phases in the as-cast samples of Ni-Ru-Zr [9-11]*

Phase	Pearson symbol / Space group	Phase range in binary system(s) /at.%	Extension in ternary /at.%
(Ni)	*cF4* / *Fm3m*	0 to 1.78 Zr / 0 to 34.5 Ru	~36 Ru / ~2 Zr
(Ru)	*hP2* / *P63/mmc*	0 to ~50 Ni / 0 to 1.9 Zr	~51 Ru / ~ 4 Zr
(βZr)	*cI2* / *Im3m*	0 to 2.92 Ni	~13 Ni / ~12 Ru
~$ZrNi_5$	*cF24* / *F43m*	14.85 to 18.40 Zr	~18 Ru
~Zr_2Ni_7	*mc36* / *I2/m*	22.2 Zr	~11 Ru
~Zr_8Ni_{21}	(*a*) / …	27.6 Zr	~19 Ru
~Zr_7Ni_{10}	*oC68* / *C2ca(b)*	41.1 to 43.22 Zr	~2 Ru
~Zr_9Ni_{11}	*tI40* / *I4/m*	45 Zr	~2 Ru
~ZrNi	*oC8* / *Cmcm*	50.1 Zr	~6 Ru
~Zr_2Ni	*tI12* / *I4/mcm*	66.7 Zr	~8 Ru
~$ZrRu_2$	*hP12* / *P63/mmc*	64 to 68 Ru	~32 Ni
~ZrRu	*cP2* / *Pm3m*	48 to 52 Ru	~20 Ni
τ_1 $Zr_{24}Ru_{22}Ni_{44}$	?	32.2-16.5 Zr / 38.0-24.0 Ru / 32.5-54.3 Ni	N/A
τ_2 $Zr_{74}Ru_4Ni_{22}$	?	76.7-73.2 Zr / 6.3-2.4 Ru / 19.5-24.3 Ni	N/A
τ_3 $Zr_{35}Ru_3Ni_{62}$	?	37.0-32.5 Zr / 1.6-3.7 Ru / 61.4-64.4 Ni	N/A

opportunity to study how hardness was related to crystal structures and compositions, phase proportions and morphology.

2. Experimental

The carbon coatings needed for SEM analysis [12] were removed by grinding, prior to XRD analyses, to obtain results without carbon. Phase proportions were calculated using the lever rule on the solidification projection for the Ni-Ru-Zr alloys [12]. A CSM® nanoindentor with an atomic force microscope (AFM) was used for nanoindentations on the individual phases. At least four indentations per phase were produced by the Berkovich type nanoindentation tip. The recorded data were displayed using image processing software.

Macro-hardness measurements were done on as-cast samples of about 2 g [12] (approximately 10 mm diameter and 7 mm thick) to obtain the hardness and identify samples with deleterious brittle phases. A Mitutoyo Hardness tester (Model AVK-CO) was used with a 10kg load, calibrated against a standard aluminium test block according to ASTM E92 [15]. Reported values were averages of at least four different indentations separated by a distance of at least three indentations' width. For each sample, images were taken at x20 objective using an optical microscope, to view as much area as possible around the indentations and discern the slip modes, and cracking to detect brittle phases.

3. Results

Selected microstructures are given in Figure 1 to show the different morphologies in the as-cast alloys [12]. Table 2 shows the nanohardness of the individual intermetallic phases, most of which had composition ranges. Unfortunately, (Ru), (Ni), and (βZr) were too small to measure individually without including the surrounding phases, so the conventional hardness values were provided instead [16]. For the nanohardness, underlying phases could have affected the analyses, since these phases were small (<7 μm across), especially for Ni_{44}:Ru_{28}:Zr_{28}, Ni_{60}:Ru_{15}:Zr_{25}, Ni_{58}:Ru_5:Zr_{37} and Ni_{36}:Ru_{13}:Zr_{51} (at.%).

The Vickers hardness is shown in Table 3. Sample 3, as-cast Ni_{20}:Ru_{60}:Zr_{20} (at.%), had the highest hardness, while Sample 6, Ni_{57}:Ru_{21}:Zr_{22} (at.%), had the lowest hardness. The indentations for the "very brittle" alloys are shown in Figure 2. The lowest hardness samples (Alloys 6 and 8, Table 3 and Figure 2) had no Palmqvist cracks from the indentation corners, and the indentations were pin-cushioned, with major slip lines. Chipping was seen in as-cast Ni_{19}:Ru_{44}:Zr_{37} (Figure 2e) and Ni_{60}:Ru_8:Zr_{32} (Figure 2f) (at.%). The Ni_{53}:Ru_{14}:Zr_{33} (at.%) alloy (Figure 2g)

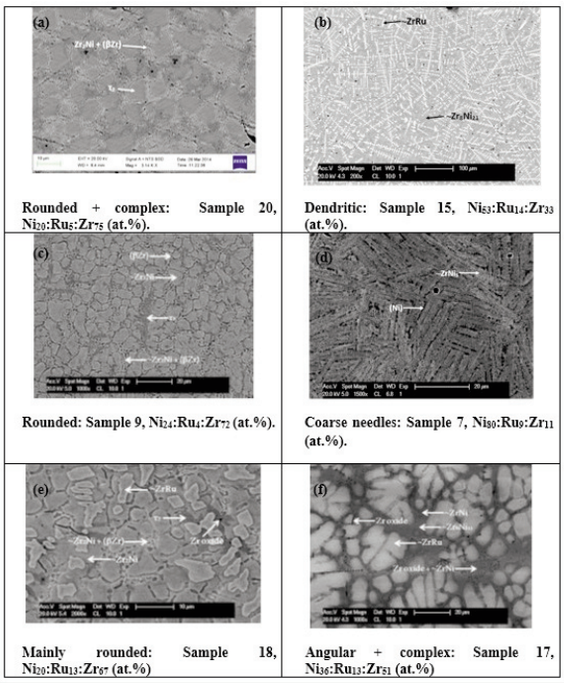

Figure 1. *SEM-BSE images showing some of the different morphologies of the different as-cast samples [12]*

Table 2. *Nanohardness for the binary and ternary phases present in the Ni-Ru-Zr alloys, and the approximate phase sizes as measured along the smallest dimension, with bulk element values [16]*

Phase	Average nanohardness /HV	Nanohardness range /HV	Approximate phase size /μm
Ru	2298 (Bulk [16])	N/A	N/A
~$ZrRu_2$	1289±23	1259 – 1315	4.2
~Zr_8Ni_{21}	1277±117	1172 – 1508	24
τ_1	1141±60	1041 –1230	100
τ_3	1012±10	1003 – 1026	16
~ZrRu	1005±7	1001 – 1015	10.0
~$ZrNi_5$	958±12	948 – 974	12
~Zr_7Ni_{10}	924±52	874 – 986	6.0
~Zr_9Ni_{11}	908±4	904 – 912	4.0
τ_2	866±16	854 – 877	7
Zr	(820 -1800 for bcc, hcp and martensite) - bulk [16])	N/A	N/A
~Zr_2Ni	785±87	684 – 888	3.0
~ZrNi	783±45	740 – 826	3.0
~Zr_2Ni_7	695±40	643 – 767	20.6
Ni	638 (Bulk [16])	N/A	N/A

had major cracking, whereas $Ni_{51}:Ru_8:Zr_{41}$ (at.%) (Figure 2h) had chipping on the cracks. The $Ni_{60}:Ru_8:Zr_{32}$ (at.%) alloy (Figure 2f) had less chipping at the circular cracks, than $Ni_{19}:Ru_{44}:Zr_{37}$ (Figure 2e) and $Ni_{53}:Ru_{14}:Zr_{33}$ (Figure 2g) (at.%). As-cast $Ni_{53}:Ru_{14}:Zr_{33}$ (at.%) (Figure 1g) had the same phases as $Ni_{60}:Ru_8:Zr_{32}$ (at.%) (Figure 2f), and both had circular ("penny") cracks. The indentations for the "brittle" alloys had corner cracking, Figure 3. Alloys $Ni_{18}:Ru_{37}:Zr_{45}$ (Figure 3a) and $Ni_{42}:Ru_{32}:Zr_{26}$ (Figure 3f) (at.%) had other cracks as well. The

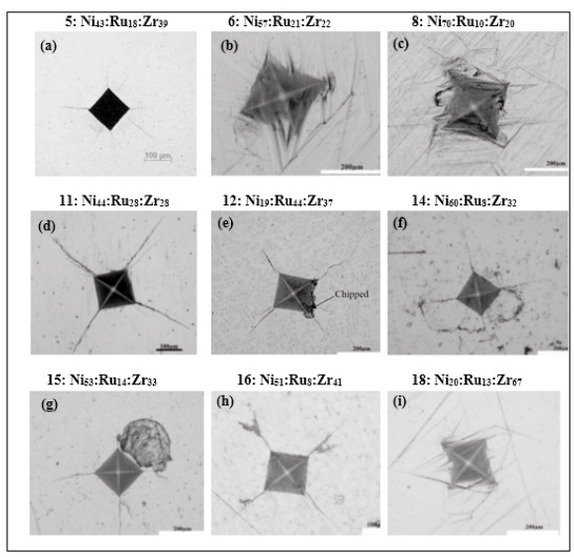

Figure 2. *Vickers hardness indentations for the "very brittle" Ni-Ru-Zr alloys, showing: f) $Ni_{60}:Ru_8:Zr_{32}$ with irregular circular cracks, g) $Ni_{53}:Ru_{14}:Zr_{33}$ with circular cracks, h) $Ni_{51}:Ru_8:Zr_{41}$ with bifurcated cracks, and i) $Ni_{20}:Ru_{13}:Zr_{67}$ (at.%) with mainly parallel slip lines*

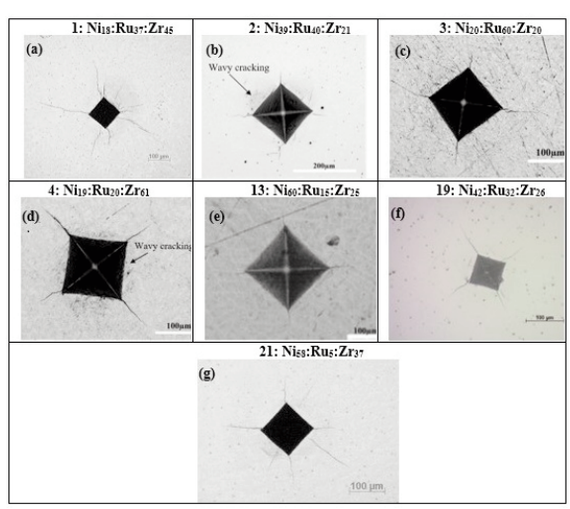

Figure 3. *Vickers hardness indentations for the "brittle" alloys in the Ni-Ru-Zr system*

Table 3. *Phases, phase proportions, cracking type and mode, relative brittleness, measured hardness and calculated hardness from phase proportions. (Hardness for Sample 1 taken at HV_5)*

Sample, nominal composition /at.%	Phases in proportion order	Phase proportions /%	Cracking type and mode	Relative brittleness	Hardness /HV_{10}, morphology	Calculated hardness from phase proportions /HV
1, Ni_{18}:Ru_{37}:Zr_{45}	~ZrRu	73	Major and wavy	Brittle	851±50	1042
	τ_1	27			Rounded	
2, Ni_{39}:Ru_{40}:Zr_{21}	τ_1	42	Minor and wavy	Brittle	832±55	1228
	~$ZrRu_2$	31			Dendrite + eutectic	
	~Zr_2Ni_7	17				
	(Ru)	10				
3, Ni_{20}:Ru_{60}:Zr_{20}	~$ZrRu_2$	67	Minor and wavy	Brittle	1015±21	1425
	τ_1	17			Rounded	
	(Ru)	16				
4, Ni_{19}:Ru_{20}:Zr_{61}	~Zr_2Ni	38	Minor and wavy	Brittle	584±7	855
	τ_2	25			Angular + complex	
	~ZrRu	20				
	(βZr)	17				
5, Ni_{43}:Ru_{18}:Zr_{39}	~Zr_7Ni_{10}	39	Major and regular	Very brittle	769±25	976
	τ_3	38			Rounded + complex	
	~ZrRu	23				
6, Ni_{57}:Ru_{21}:Zr_{22}	~Zr_2Ni_7	51	Major and irregular	Very brittle	300±19	928
	τ_1	25			Plate-like	
	~$ZrNi_5$	20				
	(Ru)	4				
7, Ni_{80}:Ru_9:Zr_{11}	~$ZrNi_5$	90	Minor, irregular and pin-cushioning	Slightly brittle	477±19	926
	(Ni)	10			Coarse needles	
8, Ni_{70}:Ru_{10}:Zr_{20}	~Zr_2Ni_7 ~$ZrNi_5$	56	Major and irregular	Very brittle	317±10	771
	(Ni)	30			Plate-like	
		14				
9, Ni_{24}:Ru_4:Zr_{72}	τ_2	77	Minor and pin-cushioning	Slightly brittle	462±19	724
	~Zr_2Ni	19			Rounded	
	(βZr)	4				

* *table continued on next page*

** table continued from the previous page*

10, Ni_{31}:Ru_9:Zr_{60}	~ZrNi	40	Minor and pin-cushioning	Slightly brittle	469±9	845
	~Zr_2Ni	23			Rounded	
	~ZrRu	22				
	τ_2	15				
11, Ni_{44}:Ru_{28}:Zr_{28}	τ_1	74	Major and regular	Very brittle	840±24	1027
	~Zr_2Ni_7	26			Dendritic	
12, Ni_{19}:Ru_{44}:Zr_{37}	τ_1	53	Major and chipping	Very brittle	844±51	1077
	~ZrRu	47			Rounded	
13, Ni60:Ru15:Zr25	~Zr_2Ni_7	62	Minor and regular	Brittle	531±9	870
	τ_1	38			Needles + eutectic	
14, Ni_{60}:Ru_8:Zr_{32}	~Zr_8Ni_{21}	98	Major and circular cracks	Very brittle	761±26	1272
	~ZrRu	2			Dendritic	
15, Ni_{53}:Ru_{14}:Zr_{33}	~Zr_8Ni_{21}	94	Major and chipping	Very brittle	841±7	1261
	~ZrRu	6			Dendritic	
16, Ni_{51}:Ru_8:Zr_{41}	τ_3	51	Major and bifurcated	Very brittle	748±16	979
	~Zr_7Ni_{10}	36			Rounded + complex	
	~ZrRu	13				
17, Ni_{36}:Ru_{13}:Zr_{51}	~ZrNi ~ZrRu ~Zr_9Ni_{11}	42	None	Tough	476±24	884
		29			Angular + complex	
		29				
18, Ni_{20}:Ru_{13}:Zr_{67}	~Zr_2Ni	51	Major and irregular	Very brittle	464±28	834
	τ_2	29			Mainly rounded	
	~ZrRu	10				
	(βZr)	10				
19, Ni_{42}:Ru_{32}:Zr_{26}	τ_1	87	Major and chipping	Brittle	743±9	1084
	~Zr_2Ni_7	13			Dendritic	
20, Ni_{20}:Ru_5:Zr_{75}	τ_2	69	None	Not brittle	555±20	844
	~Zr_2Ni (βZr)	21			Rounded	
		10				
21, Ni_{58}:Ru_5:Zr_{37}	~Zr_7Ni_{10}	69	Major and regular	Brittle	801±9	951
	τ_3	27			Rounded + complex	
	~ZrRu	4				

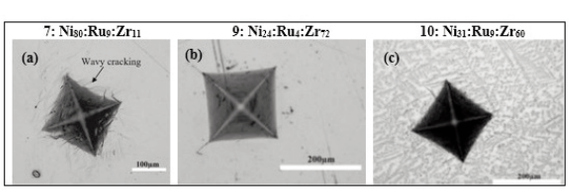

Figure 4. *Vickers hardness indentations for the "slightly brittle" alloys in the Ni-Ru-Zr system, showing pin-cushioning*

indentations for the "slightly brittle" alloys are shown in Figure 4, and all had some pin-cushioning, indicating some plastic deformation. The indentations for the alloys showing toughness are given in Figure 5.

4. Discussion

The EDX spectra had indicated no impurities in the samples [12], therefore the differences in hardness

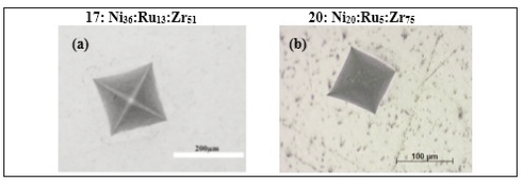

Figure 5. *Vickers hardness indentations for the tough alloys in the Ni-Ru-Zr system*

were attributed to both variation of the phase compositions, and the phases themselves. The phase nanohardness had a very wide range (Table 2), with Ru being the hardest and Ni being the least hard. The lowest Zr value of those provided [16] was assumed for the bcc phase in the samples [12]. The high Ni content of Ni_{60}:Ru_{15}:Zr_{25} (at.%) (Figure 3e) reduced brittleness, demonstrated by shorter cracks. As-cast Ni_{20}:Ru_{60}:Zr_{20} (Figure 3c) and Ni_{19}:Ru_{20}:Zr_{61} (at.%) (Figure 3d) experienced plastic deformation, shown by the wavy slip.

Dieter [17] and Shaw and DeSalvo [18] found fully work hardened materials had barrelled indentations, whereas annealed samples had pin-cushioned indentations. For as-cast samples, this implied that samples with barrelling had no more available plasticity (i.e. had reached their plasticity limit), whereas those with pin-cushioning still had plasticity. This agreed with Alloys 6 and 8 (Table 3 and Figure 2) which had no Palmqvist cracks, pin-cushioning and major slip lines, and a major phase of ~Zr_2Ni_7, the least hard compound. A similar sample was Alloy 19, which had ~ZrRu instead of ~Zr_2Ni_7.

Toughness can be approximated according to the slip lines around hardness indentations [17]. Straight slip lines indicate planar slip on the primary slip system and moderate toughness [19]; hence ~ZrRu and ~Zr_2Ni_7 were moderately tough. Wavy lines (wavy slip) indicated deformation on multiple slip systems, i.e. more plastic deformation was possible [19], as seen on Alloys 2 and 21, where ~$ZrRu_2$ (Alloy 2), and ~ZrRu (Alloy 21) were the major phases. Ranked in hardness, ~$ZrRu_2$ was second, and ~ZrRu was sixth (Table 2).

For the "very brittle" alloys, Figure 2, as-cast Ni_{43}:Ru_{18}:Zr_{39} (at.%) (Figure 2a) had indentations with straight edges, and its high brittleness could be due to high amounts of Zr oxides (dark regions within the sample). The microstructures of as-cast Ni_{57}:Ru_{21}:Zr_{22} and Ni_{70}:Ru_{10}:Zr_{20} (Figure 2b and c) had phases which were plate-like [12], and the large difference between the hardness of the different phases (Table 2) could have caused irregular hardness indentations, because slip only occurred in some phases only (~ZrRu and ~Zr_2Ni_7).

Alloy 3 (Table 3) was the only alloy with mostly ~$ZrRu_2$ (67%) was the hardest alloy, because $ZrRu_2$ was the hardest intermetallic phase (Table 2). Similarly, Alloy 6 had the lowest hardness and was mainly ~Zr_2Ni_7 (51%), which had the lowest hardness (Table 2). The τ_2 ternary phase had the lowest hardness of the ternary phases (Table 2), consistent with Table 3: Alloy 20 (mainly τ_2) was less hard than Alloy 19 (mainly τ_1) and Alloy 21 (mainly τ_3).

The brittleness of Ni_{19}:Ru_{44}:Zr_{37} (Figure 2e) and Ni_{51}:Ru_8:Zr_{41} (Figure 2h) (at.%) was attributed to τ_1 and τ_3, since ternary phases were usually brittle [20]. Although Ni_{53}:Ru_{14}:Zr_{33} (at.%) had less of the hard ~Zr_8Ni_{21} phase than Ni_{60}:Ru_8:Zr_{32} (at.%), the needle-like morphology of ~ZrRu might have increased the brittleness (more chipping) of Ni_{53}:Ru_{14}:Zr_{33} (at.%) (Figure 2g). The Ni_{51}:Ru_8:Zr_{41} (at.%) alloy had bifurcated cracks (Figure 2h) and τ_3 was the major phase (Table 3). The overall hardness of Ni_{51}:Ru_8:Zr_{41} (at.%) (with bifurcated cracks) was less than Ni_{60}:Ru_8:Zr_{32} and Ni_{53}:Ru_{14}:Zr_{33} (at.%) circular cracks (Table 3).

Since brittleness and hardness are often directly related [21], the low brittleness was attributed to the low Ru content. For higher Ru contents, the hcp crystal structure of Ru [10, 11] would increase both high hardness and brittleness. The Ni_{80}:Ru_9:Zr_{11} (at.%) alloy (Figure 4a) had irregular indentations, combining slip and cracks. Cracks probably occurred between different phases: (Ni) would slip and ~$ZrNi_5$ would be more brittle. Large differences between values of phase hardness and different morphologies (Figure 1d) could have produced the irregular hardness indentations for Ni_{80}:Ru_9:Zr_{11} (at.%). On Ni_{31}:Ru_9:Zr_{60} (at.%) (Figure 4c), cracks propagated between dendritic ~ZrRu and interdendritic ~Zr_2Ni [12].

As-cast Ni_{36}:Ru_{13}:Zr_{51} (Figure 5a) and Ni_{20}:Ru_5:Zr_{75} (at.%) (Figure 5b) had reasonable toughness: no visible cracks, pin-cushioning (indicating toughness [17, 20]), and a depression around the indentations. This was due to relatively low (Ru) contents, 13 and 5 at.% Ru, as Ru is a solid solution strengthener [3]. The Ni_{36}:Ru_{13}:Zr_{51} (at.%) sample had no brittle ternary phases, Figure 1f [12]. Conversely, Ni_{20}:Ru_5:Zr_{75} (at.%) had reasonable toughness, with about ~70% τ_2, which could have been due to its well-rounded morphology (Table 3).

With reasonable toughness (absence of cracks), Ni_{36}:Ru_{13}:Zr_{51} and Ni_{20}:Ru_5:Zr_{75} (at.%) had relatively low hardness (Table 3). However, they were harder than some brittle alloys, e.g. Ni_{57}:Ru_{21}:Zr_{22} and Ni_{70}:Ru_{10}:Zr_{20} (at.%), both of which had plate-like phases (Table 3), and the lowest hardness. Energy was lost in forming cracks, rather than in deepening the indentation [17, 18, 20], thus the hardness of cracked samples were probably under-reported.

The average samples' hardness were superposed on the solidification phases [12], Figure 6, showing the relationship between hardness, phase and

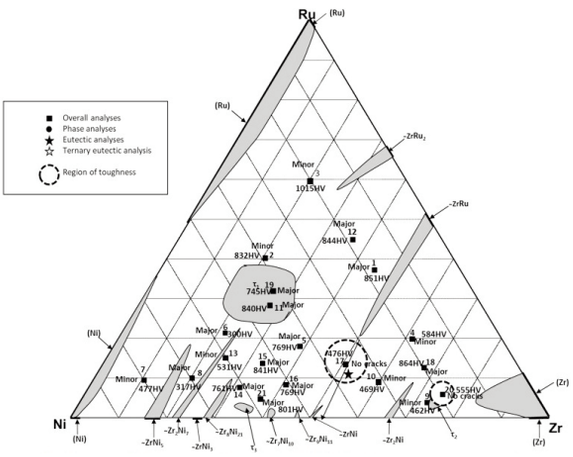

Figure 6. *Hardness (HV_{10}) and crack modes of all Ni-Ru-Zr as-cast samples (at.%)*

composition, with low hardness near the Ni-rich corner and the highest hardness towards the Ru-rich corner. As-cast Ni_{20}:Ru_{60}:Zr_{20} (at.%) had the highest hardness (1015±21 HV_{10}), consistent with the high (Ru) and ~$ZrRu_2$ proportions [6], both being hcp [10,11] with the highest phase hardness (Tables 2 and 3). The high hardness agreed with Ru additions to WC-Co [21], and Co-Ru-Pt alloys [22]. The lowest hardness (300±19 HV_{10}) was for as-cast Ni_{57}:Ru_{21}:Zr_{22} (at.%) which had very low Ru and a high Ni content, Table 2 [16]. The wide range of reported hardness for Zr [16] was due to the two different phases (α and β), and the potential of forming martensite on fast cooling [23], which did not appear to have occurred in the arc-melted samples [12].

Figure 6 also shows the different crack modes superposed on the overall composition plot. Only one as-cast sample, Ni_{36}:Ru_{14}:Zr_{50} (at.%), showed planar slip (straight edges), associated with high toughness [19]. However, it was expected that samples with

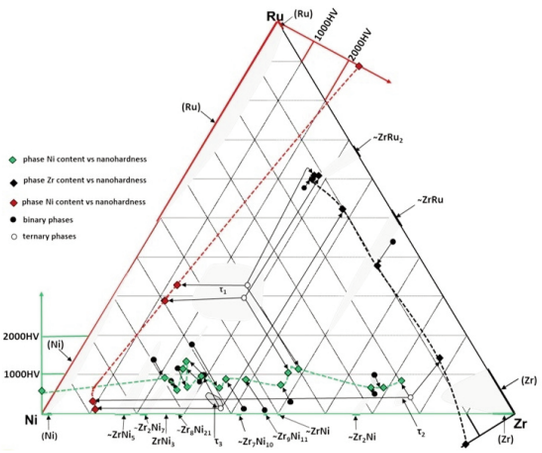

Figure 7. *Phases and their nanohardness superposed on the solidification projection for as-cast Ni-Ru-Zr alloys*

wavy slip would be tougher [19]. The Ni_{36}:Ru_{13}:Zr_{51} (at.%) sample had low hardness, ~476±24 HV_{10}, due to having mostly Ni-Zr phases, toughening the sample and no ternary phase, which are normally brittle [20]. The other tough sample, with no cracks, was Ni_{20}:Ru_5:Zr_{75} (at.%). The rest of the samples were brittle, with cracks. Some samples had wavy cracking

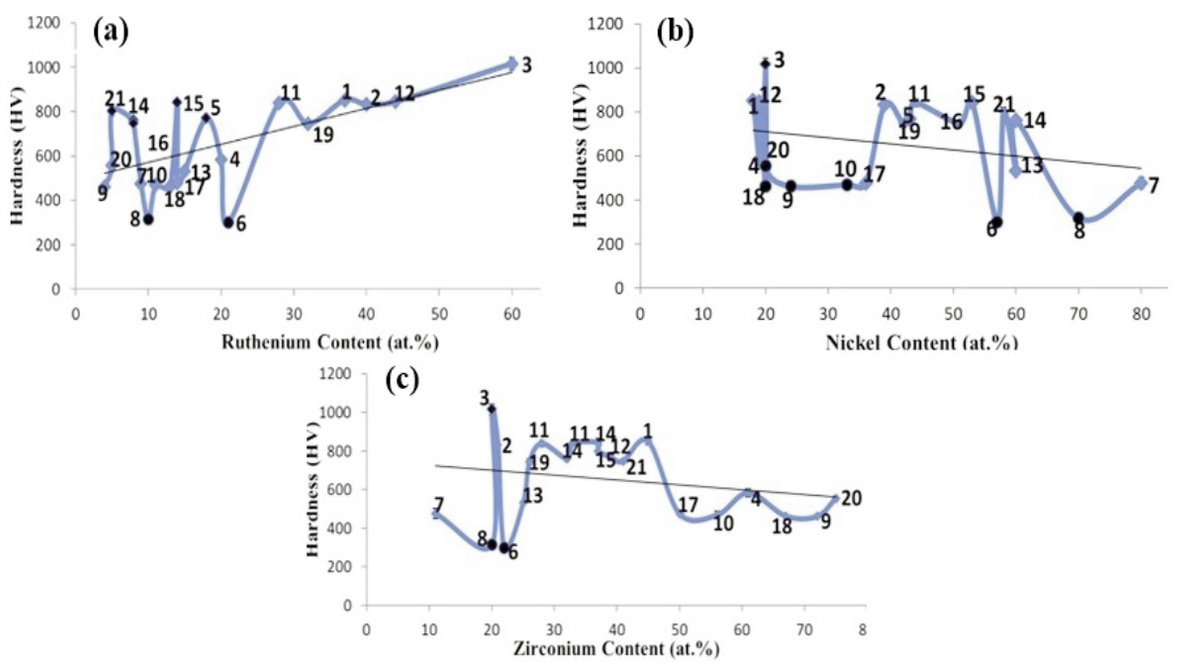

Figure 8. *Effect of: a) Ru content, b Ni content, c) Zirconium content: on alloy hardness, where black data points were significantly different from the trend line*

(deformation on multiple slip systems with much plastic deformation [19]), and hence toughness. Regions of toughness were estimated with average compositions of ~Zr_{50}:Ru_{14}:Ni_{36} and ~Zr_{75}:Ru_5:Ni_{20} (at.%), Figure 6.

It was expected that alloy hardness would lie between Ni (least hard) and Ru (hardest), but some alloys had lower hardness than Ni, which could have been due to differences in measuring conditions, e.g. the loads used, because hardness values can be load dependent [24,25]. Brittle samples which cracked, resulting in irregular indentations, had 10 - 20 at.% Ru, although the phases were not all the same. Nominal phase nanohardness (Tables 2 and 3) were superposed on the as-cast Ni-Ru-Zr phases, Figure 7, with nanohardness plotted against the corresponding binary axis, and each ternary phase plotted against all the binary axes. Generally, the phase hardness increased with ruthenium content, the hardest sample having the highest ruthenium, since Ru had the highest hardness here (Table 3). Ruthenium is a solid solution strengthener [2,21], and is also hcp with few slip systems [20]. The increasing hardness with ruthenium content is shown in Figure 8a, and Figure 8b shows that hardness decreased with increased Ni content. The latter could be due to nickel's inherent softness (fcc has 12 close packed slip systems [20]), even when it is in a non-fcc structure. A slight general decreased hardness occurred with increasing Zr content (Figure 8c), similar to Ni. Some samples had hardness higher or lower than the trend (Figure 8), due to the different crystal structures of the different intermetallic compounds and the different morphologies, Tables 4 and 5. Since this was a ternary system, there would not be a direct linear effect, as there were two independent variables (compositions of two components).

Tables 2 and 3 show that that six phases, ~ZrRu, ~$ZrRu_2$, ~Zr_8Ni_{21}, (Ru), τ_1 and τ_3, were among the hardest and were associated with more than one sample having higher hardness than the trend (Table 4). The ~ZrRu and ~Zr_8Ni_{21} phases were in both Alloys 14 and 15; the difference in hardness was due to different morphologies (Table 3) [20]. In Alloy 14, ~ZrRu was more rounded than in Alloy 15. The needle-like ~ZrRu in Alloy 15 increased hardness (Table 3). The matrix was ~Zr_8Ni_{21} in both alloys, with coring more visible in Alloy 14. Proportions of the constituent phases of Alloys 14 and 15 were similar, although the harder Alloy 15 had less of the harder phase, ~Zr_8Ni_{21}, than Alloy 14. Thus, for Alloys 14 and 15, the proportions of the constituent phases had less effect on the overall hardness than their morphologies. All the hardest samples comprised ~ZrRu or ~$ZrRu_2$ and (Ru), which was expected since (Ru) and ~$ZrRu_2$ were both hard (Tables 2 and 3), being hcp structures [10,11], with few slip systems. The ~ZrRu phase was disordered bcc [10], with many slip systems. However, the binary phases all had a third component, which had an effect. As-cast Ni_{20}:Ru_{60}:Zr_{20} (at.%), Alloy 3, had higher hardness than the trend in Figures 8b and 8c, but not in Figure 8a, because Ru had the lowest proportion (Table 3). Thus, the main effect was due to its main phase, ~ZrRu (Table 2).

Table 4. *Samples with higher hardness than the trend, with the five hardest phases in bold*

Figure	Sample number, overall composition /at.%	Phases	Morphology
8a	21, Ni_{58}:Ru_5:Zr_{37}	~Zr_7Ni_{10}, τ_3, ~ZrRu	Rounded + complex
8a	16, Ni_{51}:Ru_8:Zr_{41}	τ_3, ~Zr_7Ni_{10}, ~ZrRu	Rounded + complex
8a	14, Ni_{60}:Ru_8:Zr_{32}	~Zr_8Ni_{21}, ~ZrRu	Dendritic
8a	15, Ni_{53}:Ru_{14}:Zr_{33}	~Zr_8Ni_{21}, ~ZrRu	Dendritic
8a	5, Ni_{43}:Ru_{18}:Zr_{39}	~Zr_7Ni_{10}, τ_3, ~ZrRu	Rounded + complex
8b	3, Ni_{20}:Ru_{60}:Zr_{20}	~$ZrRu_2$, τ_1, (Ru)	Rounded
8c	3, Ni_{20}:Ru_{60}:Zr_{20}	~$ZrRu_2$, τ_1, (Ru)	Rounded

Two samples, Ni_{70}:Ru_{10}:Zr_{20} and Ni_{57}:Ru_{21}:Zr_{22} (at.%), had significantly lower hardness than the trends, Figure 8 (Table 5) because these alloys were mainly the monoclinic ~Zr_2Ni_7 phase [26], which had the lowest phase hardness (Table 2). Although ~Zr_2Ni_7 might be expected to be hard due to the fewer slip planes in monoclinic phases, the plate-like morphology in both Ni_{57}:Ru_{21}:Zr_{22} and Ni_{70}:Ru_{10}:Zr_{20} (at.%) (Table 3) probably lowered the hardness, although the ~$ZrNi_5$ phase in both samples was fcc [26], which was probably the main cause of the low hardness. The fcc (Ni) phase was also present in the Ni_{70}:Ru_{10}:Zr_{20} (at.%) sample. Alloys 9, 10, 17, and 18 also had lower values than the trend line (Figure 8c), because they comprised Ni-Zr compounds which had lower hardness than Ru-Zr compounds (Table 2). The low hardness τ_2 ternary phase (Table 2) was also associated with low hardness Alloys 9, 10, and 18 of Figure 12, where the highest proportion was in Alloy 9. In Alloys 10 and 18, τ_2 had proportions of 15% and 29%, enough to influence the overall hardness.

Although some samples showed toughness, probably the large difference in hardness of the phases (Table 2) and the very different structures mean that there was no potential for good mechanical properties in this system. The nickel-based superalloys were

Table 5. *Samples with lower hardness than the trend, with the five least hard phases in bold*

Figure	Sample number, overall composition /at.%	Phases	Morphology
8a	8, Ni_{70}:Ru_{10}:Zr_{20}	~Zr_7Ni_2, ~$ZrNi_5$, (Ni)	Plate-like
8a	6, Ni_{57}:Ru_{21}:Zr_{22}	~Zr_2Ni_7, τ_1, ~$ZrNi_5$, (Ru)	Plate-like
8b	8, Ni_{70}:Ru_{10}:Zr_{20}	~Zr_7Ni_2, ~$ZrNi_5$, (Ni)	Plate-like
8b	20, Ni_{20}:Ru_5:Zr_{75}	τ_2, ~Zr_2Ni, (βZr)	Rounded
8b	6, Ni_{57}:Ru_{21}:Zr_{22}	~Zr_2Ni_7, τ_1, ~$ZrNi_5$, (Ru)	Plate-like
8b	18, Ni_{20}:Ru_{13}:Zr_{67}	~ZrNi, ~Zr_2Ni, ~ZrRu, τ_2	Mainly rounded
8b	9, Ni_{24}:Ru_4:Zr_{72}	τ_2, ~Zr_2Ni, (βZr)	Rounded
8b	10, Ni_{31}:Ru_9:Zr_{60}	~ZrNi, ~Zr_2Ni, ~ZrRu, τ_2	Rounded
8b	17, Ni_{36}:Ru_{13}:Zr_{51}	~ZrNi, ~ZrRu, ~Zr_9Ni_{11}	Angular + complex
8c	8, Ni_{70}:Ru_{10}:Zr_{20}	~Zr_2Ni_7, ~$ZrNi_5$, (Ni)	Plate-like
8c	6, Ni_{57}:Ru_{21}:Zr_{22}	~Zr_2Ni_7, τ_1, ~$ZrNi_5$, (Ru)	Plate-like

based on two phases which were similar: fcc (Ni) and $L1_2$ ~Ni_3Al [8] which had similar hardness [27]. Even if the samples had been annealed, the wide range of hardness and structures might still not have given good properties.

5. Conclusions

Most of the phases had their nanohardness measured on single-phase areas, and the hardness of the phases were ranked: Ru > ~$ZrRu_2$ > ~Zr_8Ni_{21} > τ_1 > τ_3 > ~ZrRu > ~$ZrNi_5$ > ~Zr_7Ni_{10} > ~Zr_9Ni_{11} > τ_2 > Zr > ~Zr_2Ni > ~ZrNi > ~Zr_2Ni_7 > Ni. The as-cast Ni_{20}:Ru_{60}:Zr_{20} (at.%) sample had the highest hardness, and as-cast Ni_{57}:Ru_{21}:Zr_{22} (at.%) had the lowest hardness. Increased Ru content resulted in increased hardness of the as-cast samples. Most of the Ni-Ru-Zr samples were brittle, except for as-cast Ni_{36}:Ru_{13}:Zr_{51} and Ni_{20}:Ru_5:Zr_{75} (at.%) which showed crack-free indentations, thus the surrounding regions were estimated to be the regions of toughness in the Ni-Ru-Zr system. Since there were only two moderately tough regions, there is a low potential for further development for good mechanical properties.

References

[1] C.Y. Cui, Y.F. Gu, D.H. Ping, H. Harada, M. Osawa, A. Sato, Metall. Mater. Trans. A, 37 (2) (2006) 355-360.

[2] T. Biggs, P.J. Hill, L.A. Cornish, M.J. Witcomb, J. Phase Equilibria., 22 (3) (2001) 214-218.

[3] M.J. Stern, H. Wissenburg, J. Electrochem. Soc., 106 (9) (1959) 759-764.

[4] N.D. Green, C.R. Bishop, M. Stern, J. Electrochem. Soc., 108 (9) (1961) 836-841.

[5] S. Floreen, J.M. Davidson, Metall. Trans. A., 14 (4) (1983) 895–901.

[6] R.L. Fleischer, R.J. Zabala, R.J., Metall. Mater. Trans. A., 21 (1990) 2709–2715.

[7] R.L. Fleischer, ISIJ Int., 31 (10) (1991) 1186-1191.

[8] R.C. Reed, The Superalloys: Fundamentals and Applications, Cambridge University Press, Cambridge, 2008, p. 33-120.

[9] A. Jana, S. Sridar, S.G. Fries, T. Hammerschmidt, K.C. Hari Kumar, Intermetallics, 116 (2020) 106640.

[10] N. David, T. Benlaharche, J.M. Firorani, M. Vilasi, Intermetallics, 15 (2007) 1632-1637.

[11] S. Hallström, D. Andersson, A. Ruban, J. Ågren, Acta Mater., 56 (2008) 4062–4069.

[12] L. Chipise, B.O. Odera, P.K. Jain, S.H. Coetzee, N.R. Batane, M.P. Motsamai, L.A. Cornish, J. Phase Equilib. Diff., 37 (6) (2016) 702-717.

[13] D.G. Pettifor, J. Phys. C, 19 (1986) 285-313.

[14] P.J. Hill, N. Adams, T. Biggs, P. Ellis, J. Hohls, S.S. Taylor, I.M. Wolff, Mater. Sci. Eng., A, 329 (2002) 295–304.

[15] Standard, A.S.T.M, ASTM E92-16, ASTM, 82 (2016) p. 1-27.

[16] G.V. Samsonov, Mechanical Properties of the Elements, Handbook of the Physicochemical Properties of the Elements, Springer US, New York, 2009, p. 387-446.

[17] G.E. Dieter, Mechanical Metallurgy, SI Metric Edition., McGraw-Hill, London, 1990 p. 325.

[18] M.C. Shaw, G.J. DeSalvo, Metallogr. Microstruct. Anal., 1 (6) (2012) 310-317.

[19] R. Suss, Investigation of the Pt-Al-Cr System as Part of the Development of the Pt-Al-Cr-Ru Thermodynamic Database, PhD Thesis, University of the Witwatersrand, Johannesburg, South Africa, 2007.

[20] D.R. Askeland, P.P. Fulay, W.J. Wright, The Science and Engineering of Materials, SI 6th Edition, Springer, US, New York, 2010, p. 86-479.

[21] T.L. Shing, S. Luyckx, I.T. Northrop, I. Wolff, Int. J. Refract. Met. Hard Mater., 19 (1) (2001) 41-44.

[22] L. Glaner, A Study of the Ni-Pt-Ru and Co-Pt-Ru Systems, MSc Dissertation, University of the Witwatersrand, Johannesburg, South Africa, 2009.

[23] K. Chen, L. Zeng, Z. Li, L. Chai, Y. Wang, L.Y. Chen, H. Yu, J. Alloy Compd., 784 (2019) 1106-1112.

[24] D. Chakraborty, J. Mukerji, J. Mater. Sci., 15 (12) (1980) 3051-3056.

[25] K. Hirao, M. Tomozawa, J. Am. Ceram. Soc., 70 (1987) 497-502.

[26] S.A. Pogodin, V.I. Sokorobotogatova, Izv. Sekt. Fiz-Khim. Anal., Inst. Obshch. Khim. Akad. Nauk SSSR, 25 (1954) 70-80.

[27] E. Nikulina, K. Durst, M. Göken, R. Völkl, U, Glatzel, Int. J. Mat. Res., 101 (2010) 585-588.

KARAKTERISTIKE TVRDOĆE KOD LIVENIH Ni-Ru-Zr LEGURA

L. Chipise [a-d,*], N.R. Batane [b,d], P.K. Jain [b,e], S.H. Coetzee [b,f], B.O. Odera[b,g], W. Goosen[h], L.A. Cornish [a,b]

[a] Vitvatersrand univerzitet, Hemijsko-metalurški fakultet i DST-NRF centar za izvrsnost čvrstih materijala, Johanesburg, Južna Afrika
[b] Afrička mreža za nauku o materijalima (AMSEN: A Carnegie–IAS RISE Network)
[c] Državni univerzitet primenjenih nauka u Manikalendu, Mutare, Zimbabve
[d] Univerzitet u Bocvani, Mašinski fakultet, Gaborone, Bocvana
[e] Univerzitet u Bocvani, Fakultet za fiziku, Gaborone, Bocvana
[f] Institut za tehnološka istraživanja i inovacije u Bocvani, Gaborone, Bocvana
[g] Tehnološki univerzitet u Keniji, Fakultet za mašinsko i procesno inženjerstvo, Najrobi, Kenija
[h] Univerzitet Nelson Mendela, Centar za prenosnu elektronsku mikroskopiju visoke rezolucije, Port Elizabet, Južna Afrika

Apstrakt

U ovom radu je ispitivana tvrdoća po Vikersu kod 21 uzorka livene Ni-Ru-Zr legure različitog sastava, a otisci za utvrđivanje nanotvrdoće su dobijena za pojedinačne faze. Rezultati su korišćeni za objašnjenje krtosti materijala procenom proporcija faza i njihove morfologije. Tvrdoća jedinjena je varirala između 704 -1,289 HV, gde je ~$ZrRu_2$ bila faza sa najvećom tvrdoćom, a ~Zr_2Ni_7 faza sa najmanjom tvrdoćom. Tvrdoća uzorka je iznosila 300 – 1,015 HV. Većina uzoraka je bila krta, iako se oko Ni_{36}:Ru_{13}:Zr_{51} i Ni_{20}:Ru_5:Zr_{75} (at.%) moglo uočiti područje koje je imalo žilavost. Nije utvrđena ni jedna legura koja bi potencijalno imala dobra mehanička svojstva.

Ključne reči: *Tvrdoća; Ni-Ru-Zr; Legure; Trojni sistemi; Livene legure*